JOURNAL OF MATERIALS SCIENCE: MATERIALS IN MEDICINE 7 (1996) 141–148

Steric stabilization and cell adhesion

C. FOA, M. SOLER, A.-M. BENOLIEL, P. BONGRAND
INSERM U 387, Laboratoire d'Immunologie, Hôpital de Sainte-Marguerite, BP 29, 13274 Marseille Cedex 09, France

We present theoretical and experimental arguments supporting the hypothesis that the cell surface glycocalyx may negatively regulate adhesive phenomena. First, it is recalled that a repulsive interaction of several thousands of piconewtons may be generated on a contact area of about 1/100 μm^2 by a combination of electrostatic and entropic forces (steric stabilization). Second, electron microscopical data are reported to provide an estimate of the thickness of the cell coats of murine macrophages and sheep erythrocytes made phagocytable by exposure to glutaraldehyde or specific antibodies. Using conventional carbohydrate staining procedures, it is shown that the total thickness of the electron-dark regions in areas of intercellular contact is lower than the sum of the thicknesses of electron-dark regions on free cell areas. Further, removing negative charges with neuraminidase or neutralizing these charges with polylysine may reduce intermembrane distance in contact areas. Third, it is shown that a decrease of erythrocyte surface charges with neuraminidase increases their adhesion to murine phagocytes under dynamic, not static conditions. It is concluded that a major determinant of steric stabilization is the relative length of adhesion molecules and surface repeller elements, and that repulsion is particularly important under dynamic conditions. Thus, dynamic effects must be included in models of steric stabilization.

1. Introduction

The idea of applying basic physical chemical laws to explain cell adhesion is not new. Indeed, a quarter of a century ago, when the DLVO theory succeeded in explaining many properties of colloid suspensions, cell biologists and physical chemists attempted to apply similar concepts to biological systems [1, 2]. Although the DLVO theory could in principle account for weak and strong adhesion, even some kind of specificity [3], it was rapidly apparent that cell adhesion was mainly dependent on the presence on cell surfaces of a variety of dedicated adhesion molecules, including integrins, selectins, cadherins or members of the immunoglobulin superfamily [4, 5].

However, several lines of evidence support the concept that cell adhesion may be negatively regulated by non-specific repulsive interactions involving various components of the cell surface.

First, in some cases, cell–cell adhesion may not occur despite the presence of specific ligand and receptors on interacting surfaces. Thus, a subclass of T lymphocytes bear thousands of CD8 molecules that can bind to class I major histocompatibility complex molecules that are ubiquitous in living organisms [6]. However, these lymphocytes do not exhibit obvious adhesion to all cells they encounter. Similarly, although T lymphocytes bear CD2 molecules on their surface, they may not adhere to surfaces coated with LFA-3, a ligand of CD2 [7]. As will be suggested below, the relative inability of some ligand–receptor couples to bind when cell-to-cell approach proceeds under dynamic conditions [8, 9] may be ascribed to similar causes.

Second, whereas purely electrostatic repulsion is a rather inefficient way of preventing colloid flocculation in concentrated electrolyte solutions such as biological media, this flocculation may be efficiently prevented by coating particles with soluble polymers. The importance of this phenomenon, called steric stabilization, was emphasized by Napper [10, 11] and many basic principles were clarified by de Gennes [12, 13].

Third, it was recognized that essentially all cells were surrounded by a carbohydrate-rich atmosphere that could be stained with standard reagents (phosphotungstic acid, periodic acid and Schiff's reagent, ruthenium red, Alcian blue; see [14] for a review). This region, that appeared as an electron-light exclusion zone in the absence of specific stain, was called the "glycocalyx" by Bennett [15] and may be more frequently referred to as the "pericellular matrix" in recent papers. Note that this structure shares many components with the "extracellular matrix", which may make difficult an accurate definition of the cell boundary.

These data led Bell and Bongrand [16–19] to estimate the expected order of magnitude of steric repulsions in biological systems and emphasize the potential importance of this phenomenon.

In the present paper, we briefly review the theoretical basis of this concept. Then, we describe recent experimental results on (i) the electron microscopical

0957–4530

structure of the glycocalyx in contact areas and (ii) the role of this structure in static and dynamic adhesion.

2. Theory

2.1. Significance of forces at the cellular level

Before we give some estimates of the order of magnitude of cell–cell repulsive forces, it is useful to ask which force is indeed required to inhibit adhesion. This is obviously dependent on the conditions of cell–cell encounter:

(i) In the simplest experimental setup, contact is obtained by sedimentation. The driving force is thus of the order of a few pN [17, 18]. If centrifugation is performed, this may be increased by a factor of 1000.

(ii) If cells are considered as rigid bodies with thermal energy of order kT (k is Boltzmann's constant and T is the absolute temperature), they may overcome a repulsive barrier of width w if the force is less than kT/w. Tentatively setting w at 10 nm (see below), the corresponding force is 0.4 pN.

(iii) Now, adherent cells may send forward lamellipodia with a pushing strength of several tens of thousands of pN [20]. This probably sets a maximum to the repulsion that can be overcome in view of forming adhesions. The force likely to be exerted by a cell surface protrusion is much more difficult to evaluate.

Thus, a repulsive force lower than 1 pN is not likely to impair cell adhesion under any circumstances. A repulsion higher than about 10 000 pN will probably prevent adhesion under any conditions.

2.2. Models for the cell surface

2.2.1. Contact area

As will be shown, the most difficult part of an estimate of surface repulsions is probably to guess what the cell surface looks like. A first point is that cells do not resemble smooth spheres at the molecular level. They are known to possess an excess membrane area made of multiple folds, protrusions, microvilli, lamellipodia, with a highly dynamic behaviour. As previously mentioned [18], many authors agree that the typical thickness of these structures is of the order of 0.1 μm. Since lamellipodia are not expected to have a straight leading edge, and it is unlikely that two lamellipodia will encounter each other with parallel boundaries, the typical area of the first encounter between two cells, and probably between a cell and a flat surface, may be of the order of 0.01 μm^2.

2.2.2. Adhesion molecules

The structure of many adhesion molecules is now well known. In particular, electron microscopic studies gave valuable information on the overall molecular shape of molecules such as immunoglobulins [21], integrins [22], or ICAMs [23]. The potential importance of length differences between various adhesion molecules was emphasized in a recent review by

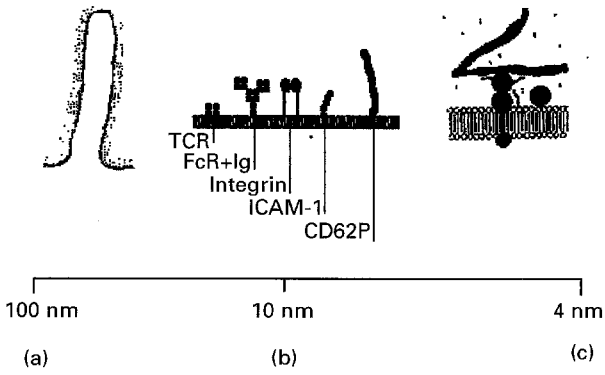

Figure 1 The cell surface. Typical details of cell plasma membranes were drawn with different scales: (a) typical microvillus with surface bound sugars (each dot represents a hexasaccharide group); (b) size of typical adhesion molecules. TCR: T cell receptor; FcR + Ig: Fcγ receptor (e.g. CD16 or CD32) bound to an IgG molecule; ICAM-1: intercellular cell adhesion molecule 1, a ligand of LFA-1 and MAC 1 (CD11a/CD18 and CD11b/CD18) integrins; CD62P: P selectin; (c) the V-shape molecule may be fibronectin.

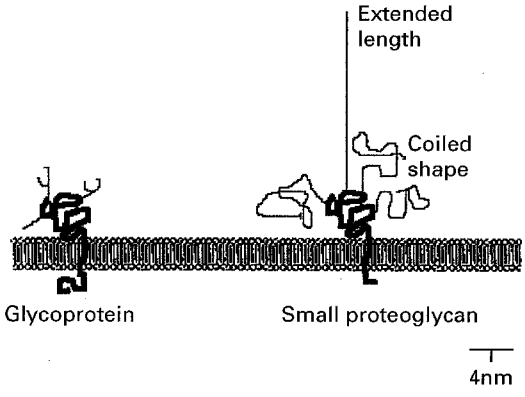

Figure 2 Components of the glycocalyx. A glycoprotein with typical oligosaccharide chains (narrow strands) is shown on the left. A small proteoglycan described on hepatocytes is shown on the right. The saccharide chains are much longer than those of glycoproteins. They may be more or less extended depending on the linear density of charged groups such as sulphate.

Springer [4] who drew to scale many binding molecules of the immune systems. Examples are shown in Fig. 1. The length of a receptor may range from 6–8 nm (CD4, CD8, CD2, LFA-3) to 40 nm (P-selectin). These differences may have high functional significance, particularly if the thickness of the cell surface repulsive layer lies between these values.

2.2.3. Modelling the glycocalyx

Although de Gennes elaborated a very useful framework to describe different configurations of surface-bound polymers (see [13] for a brief summary), it is difficult to propose a unique scheme of surface structure. It is likely that the outer membrane layer is made of carbohydrate-rich material, including oligosaccharide chains of glycoproteins (typically 10 residues per chain, 5 nm per residue) and longer chains of proteoglycans (see Fig. 2: an intrinsic proteoglycan with 4 chains of about 70 residues was found on the hepatocyte membrane). As another example, CD43,

a sialic-acid-rich membrane leukocyte surface molecule looks like a rod of 45 nm length [24]. Its orientation with respect to the bilayer is not known. There are several points of additional complexity:

(i) A given molecule may act as both a repeller and an adhesion structure. Thus, CD43 was reported to bind to ICAM-1, an adhesion molecule belonging to the immunoglobulin superfamily [25]. The neural cell adhesion molecule NCAM-1 may bear large chains of polysialic acid increasing its molecular radius from 12 nm to 17 nm, resulting in marked steric inhibition of cell-to-cell approach [26].

(ii) The conformation of the cell surface polysaccharides is not always known. They may behave as coiled structures, with a radius proportional to the 0.6 power of the number of monomers [27]. Alternatively, they may be extended if the charge density is sufficient.

(iii) In addition to intrinsic molecules inserted in the plasma bilayer, the cell surface may be coated by various structures bound by specific receptors or cooperative non-specific interactions. For example, it is not clear whether fibronectin bound to surface integrins may play a repulsive role in some situations.

2.2.4. Estimation of forces

The electrostatic repulsion between two cells bearing realistic surface charge densities (1.6×10^{-2} C/m^2; i.e. 10^5 electronic charges/μm^2) was calculated using (i) a standard DLVO approach with 2-D distribution of surface charges and (ii) assuming a constant volume distribution of charges in a region of 10 nm thickness [17, 18]. As shown in Fig. 3, calculated repulsion was markedly dependent on the selected model. Steric stabilization was also estimated by modelling polysaccharide chains as polymer molecules with a surface density of about 1 hexose unit per nm^2 and about 100 residues per chain (see [28] for a discussion of this assumption). Excluded volume effects were neglected. Repulsion could thus be calculated with analytic formulae obtained by Dolan and Edwards [29]. A simplified formula was suggested by Israelachvili [30]. The expected repulsion due to rigid molecular rod was also calculated for comparison. As shown in Fig. 4, steric stabilization may account for a substantial repulsion between cell surfaces. However, the influence of this force on adhesion is critically dependent on the relative size of adhesion molecules and glycocalyx elements.

In view of previously reported differences between static and dynamic adhesion, it was of obvious interest to estimate the potential role of dynamic repulsive interactions in cell–cell adhesion.

2.2.5. Hydrodynamic repulsion

The first interaction we consider is purely hydrodynamic. When two parallel surfaces approach each other, viscous forces may hamper the thinning of the separating liquid film [17, 31, 32]. The force

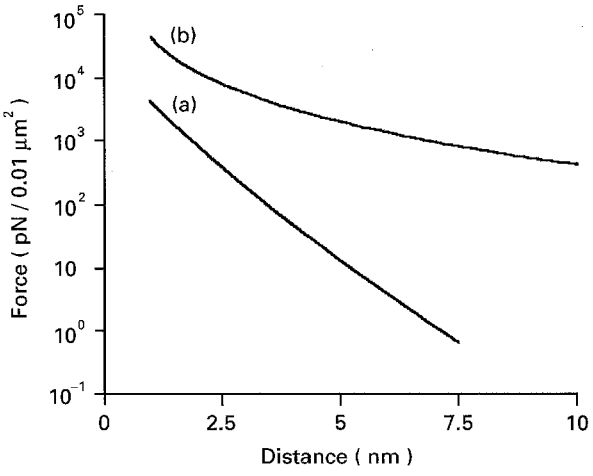

Figure 3 Electrostatic repulsion between charged membranes. The distance dependence of the repulsive force between surfaces bearing negative charges with a density matching that of biological membranes was calculated assuming (a) surface distribution and (b) volume distribution of these charges [17].

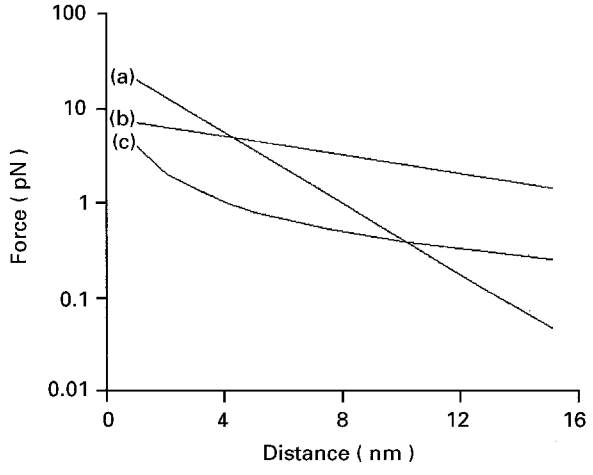

Figure 4 Steric stabilization. The distance dependence of the repulsive force between surfaces bearing grafted polymer molecules was calculated with three different models. (a) 100 chains with 100 segments of 0.5 nm length each [28], using reported analytical formulae with excluded volume neglected [29]. (b) Same model, 25 chains of 400 segments each. (c) 100 rigid rods of 15 nm length. The entropy per chain varies as $k \ln(d/L)$ where L is the chain length, d the distance between surfaces and k is Boltzmann's constant.

between parallel discs of radius a and distance d may be approximated as [32]:

$$F = (3/2)\pi\mu a^4/d^3 \, \mathrm{d}d/\mathrm{d}t \qquad (1)$$

where μ is the medium viscosity. Assuming that a is 50 nm (corresponding to the tip of microvilli) and d is 10 nm with a decrease rate of 10 μm/s, the force is 0.3 pN. However, the effective viscosity may be substantially increased by macromolecules located between approaching surfaces.

2.2.6. Polymer compression

Considering a model of isolated polymer chains and applying Kirkwood's approximation ([13], p. 173), the

repulsion generated by chain compression is:

$$F = 6\pi\mu R_g \, dd/dt \quad (2)$$

where R_g is the radius of gyration. Assuming that a microvillus bears 100 chains of 5 nm radius of gyration (corresponding to a random coil with 100 units of 0.5 nm length; see [28]) and dd/dt is 10 μm/s, F is 0.1 pN. This value is fairly low, but entanglement effects between interacting macromolecules may lead to substantial increase of this value.

2.2.7. Diffusion

Since the diffusion coefficient of pericellular matrix elements such as fibronectin is expected to be low [33], it is not known whether repellers may leave adhesion areas during cell–cell encounters if approach is fairly rapid. Clearly, more experimental data are required to assess the molecular distribution of sugar molecules in cell–cell interaction areas.

3. Materials and methods

Experimental procedures have been described elsewhere. Only a brief presentation will be given.

3.1. Cells

Phagocytes were P388D1 macrophage-like murine tumour cells of DBA/2 origin. Sheep red cells were provided by Biomérieux (Lyon, France). Immunoglobulin-coated sheep red cells (IGSRC) were prepared by incubating 2% erythrocyte suspensions in 1/100 polyclonal rabbit anti-sheep erythrocytes antiserum (IgG fraction, Sigma, St Louis, USA). Glutaraldehyde-treated erythrocytes (GSRC) were obtained by 24 h exposure to 2.5% glutaraldehyde at room temperature under continuous agitation. IGSRC and GSRC were readily bound and ingested by phagocytes at 37 °C [34] whereas only the adhesion step proceeded at room temperature (24 °C). In some cases, erythrocytes were treated with 30 or 300 U/ml neuraminidase (Tebu) to remove sialic acid for 30 min at room temperature in pH 7.2 phosphate buffer.

3.2. Static adhesion and electron microscopy

Two hundred microlitres of a suspension of P388D1 cells (5×10^6 per ml) and erythrocytes (10^7/ml) in pH 7.2 cacodylate buffer were subjected to centrifugation in an ependorf centrifuge. This was performed for 20 s at 227g ("weak centrifugation") or 2 min at 3500g ("strong centrifugation"). Pellets were then fixed with 2.5% glutaraldehyde, then 1% osmium tetroxide.

In some cases, two procedures were performed to stain the pericellular coat [35]. Ruthenium red was used at 0.05%. This reagent is a hexavalent cation that interacts with polyanions and was first used by Luft [36] to label cell surface sugars. Alcian blue, a cationic dye, was alternatively used at 0.5% concentration (see [35] for more details). Samples were finally embedded in epon. Ultrathin sections were counterstained with uranyl acetate and lead citrate for morphological observations done in absence of ruthenium red or Alcian blue treatment.

Electron micrographs (25 000× magnification) were then digitized with a Logitech Handscanner (Logitech Inc., Hsinchu, Taiwan) allowing 400 dpi resolution with 256 grey levels. Images were then processed with a specific software written in the laboratory in order to allow manual determination of cell boundaries [35] and immediate calculation of the mean thickness of delimited areas. Our analytical procedure was also used to study previously described electron micrographs prepared by Dr A. Ryter (Institut Pasteur, Paris) on rat macrophages having bound glutaraldehyde treated erythrocytes, or erythrocytes that had been subjected to both glutaraldehyde treatment and charge reduction by neuraminidase or polylysine [37].

3.3. Dynamic adhesion

Our apparatus was fully described in previous reports [38, 39]. Briefly, macrophages were deposited on a glass coverslip constituting the bottom of a parallel-plate flow chamber (17 × 6 × 1 mm). The flow was generated with an electric syringe holder (Razel Scientific, Samford, CT, USA, supplied by Bioblock, France, Ref. K88906) allowing wide variations of the flow rate (100× range). The chamber was set on the stage of an inverted microscope (Olympus IM) equipped with a 100× lens and an SIT videocamera (Model 4015, Lhesa, Cergy Pontoise, France). Each experiment was recorded with a Mitsubishi HS3398 tape recorder. All experiments were replayed in order to determine (i) the number of erythrocytes passing in contact with macrophages in a given microscope field during a standard period of 10 min, and (ii) the number of erythrocytes remaining stuck at the end of the experiment.

4. Results

4.1. Structural studies

The principle of our study was to evaluate the thickness of the cell coat in contact zones between adherent cells. We used two alternative procedures for sample preparation. With conventional fixation, the cell coat appeared as a transparent area between osmiophilic bilayers in cell–cell contact areas. However, it was invisible on free membrane areas (Fig. 5a). Alternatively, when surface carbohydrates were positively stained with ruthenium red or Alcian blue, the cell coat was visible in free and adherent areas. However, it could not be distinguished from the bilayer (Fig. 5b and c).

4.1.1. Conventional staining

In a first series of measurements, we studied the effect of electrostatic charges on the intermembranar distance in areas of contact between bound erythrocytes and macrophages. Since cells are known to bear a net

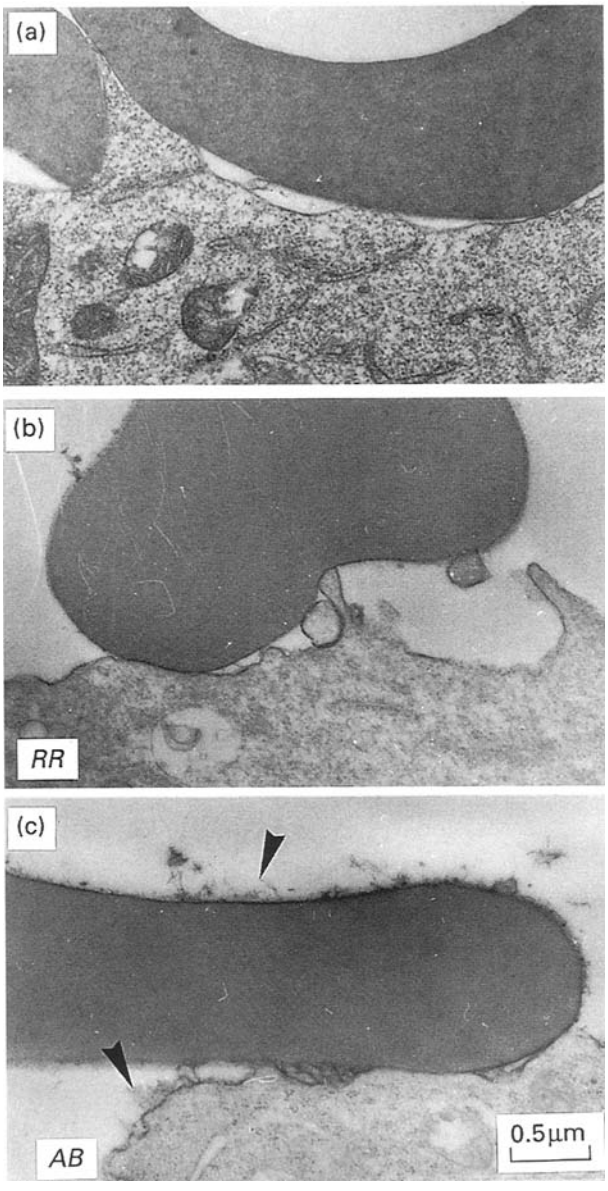

Figure 5 Electron microscopical aspect of macrophage–erythrocyte contact. (a) A typical image of an immunoglobulin-coated erythrocyte bound by a P388D1 cell is shown. The glycocalyx appears as an electron light region between apposed osmiophilic bilayers; (b) staining with ruthenium red. The apparent membrane thickness is markedly increased; (c) staining with Alcian blue. Cell surface contours are more irregular (arrows).

negative charge, sheep erythrocytes were treated with neuraminidase (to remove negative sialic groups) or polylysine (to add positive charges). Both treatments were shown to very significantly reduce the net negative charge of these erythrocytes [40]. These cells were then treated with glutaraldehyde and incubated with rat macrophages that readily bound them. Samples were then examined with electron microscopy for quantitative determination of the interbilayer distance. As shown in Table I, both neuraminidase and polylysine treatments reduced the average interbilayer distance in contact areas.

In order to get more information on the significance of our results, we determined the pixel-per-pixel distribution of interbilayer distances in contact areas (Fig. 6). As shown in Fig. 6b, neuraminidase markedly reduced the frequency of points with apparent contact

TABLE I Width of the electron-light gap between macrophages and opsonized erythrocytes

Erythrocyte treatment	Mean apparent gap width (nm)
Glutaraldehyde	21.5 ± 0.5 ($p = 2439$)
Glutaraldehyde + neuraminidase	18.1 ± 0.65 ($p = 2494$)
Glutaraldehyde + polylysine	11.7 ± 0.25 ($p = 2831$)

Control, neuraminidase-treated or polylysine-coated erythrocytes were treated with glutaraldehyde and incubated with rat macrophages that readily bound them. Samples were processed with electron microscopy and micrographs were digitized and analysed for determination of the mean distance between electron-dense bilayers in contact areas. Mean values are shown ± standard error of the mean. Each value was determined from about ten micrographs. Total number of pixels of examined contour in brackets.

between electron-dense bilayers. As shown in Fig. 6c, polylysine treatment decreased the minimum distance somewhat less efficiently, but resulted in uniformly tight apposition of bilayers.

4.1.2. Positive carbohydrate staining

We determined the average thickness of the electron-dense layer limiting macrophages and erythrocytes after staining with ruthenium red or Alcian blue. As shown in Table II, both cell types displayed similar thickness of their surface layer. However, Alcian blue labelling resulted in significantly thicker and more irregular layers (Fig. 5c). The total thickness of apposed membrane couples was then measured in contact areas. As shown in Table III, this thickness was significantly lower than the sum of the thicknesses of individual membranes, suggesting that adhesion required either intermingling or compression of cell surface layers.

4.2. Functional studies

In order to assess the significance of morphological studies, it was of obvious interest to determine whether a decrease of the pericellular coat thickness was correlated to an increase of binding efficiency.

First, it was shown in previous reports that neuraminidase or polylysine treatment of erythrocytes before glutaraldehyde modification dramatically increased the efficiency of adhesion between these erythrocytes and macrophages [40] under static conditions.

Second, neuraminidase treatment of sheep red blood cells before antibody coating did not increase their capacity to be bound by macrophages (Table IV).

Third, when immunoglobulin-coated erythrocytes were driven along phagocyte monolayers, in a flow chamber operated at very low shear rate (the wall shear rate was about 1 s^{-1}), no adhesion was found (Table V). However, a neuraminidase treatment that was unable *per se* to induce adhesion made antibody-coated erythrocytes able to bind to phagocytes under dynamic conditions. Thus, neuraminidase treatment increased the binding of glutaraldehyde-treated

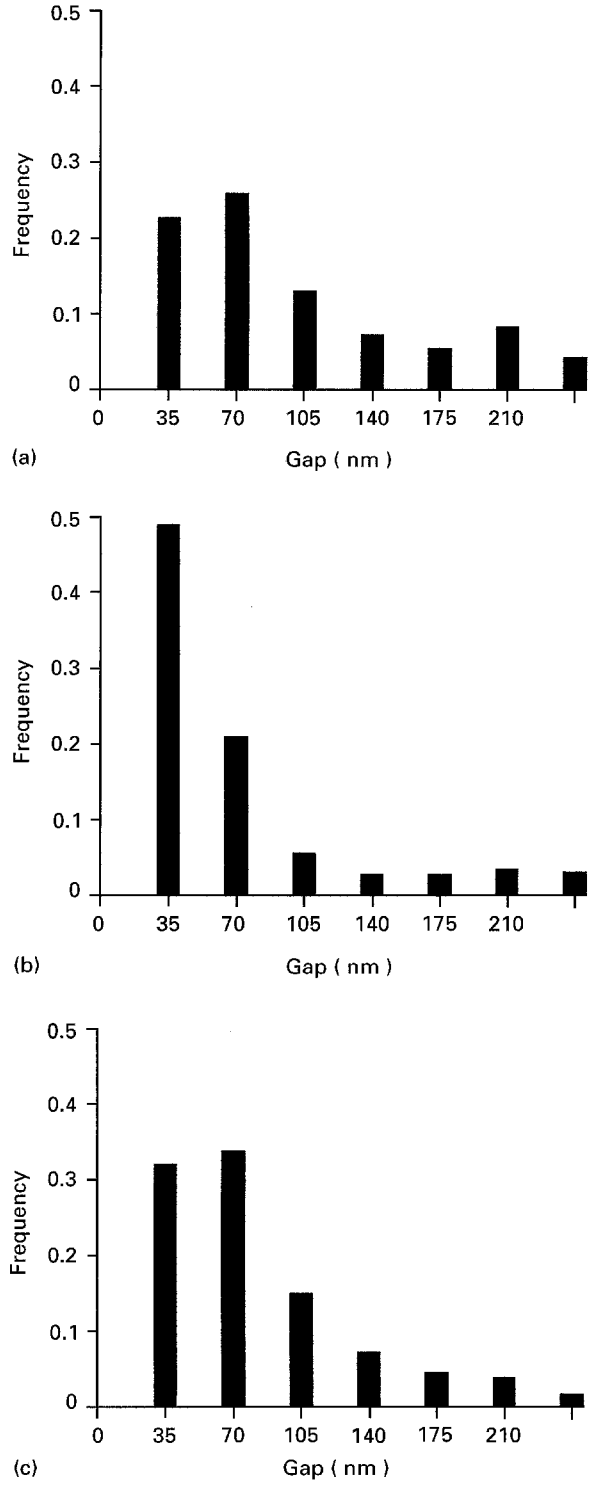

Figure 6 Rat macrophages were made to bind (a) glutaraldehyde-treated erythrocytes, (b) erythrocytes treated with neuraminidase, then glutaraldehyde, and (c) erythrocytes treated with glutaraldehyde, then polylysine. Electron micrographs were used to determine the distribution of distances between osmiophilic layers in contact areas (photographs prepared by Dr A. Ryter as explained in [37]).

erythrocytes under static conditions, and enhanced the binding of immunoglobulin-coated erythrocytes under dynamic, not static, conditions.

5. Discussion

The first goal of this paper was to present a theoretical discussion of the relevance of steric stabilization to cell

TABLE II Apparent thickness of cell membranes after carbohydrate staining

Staining procedure	Cell type	Apparent membrane thickness (nm)
Ruthenium red	Erythrocyte	15.1 ± 1.1 (n = 46, 5041 points)
Ruthenium red	P388D1	18.5 ± 1.4 (n = 49, 4871 points)
Alcian blue	Erythrocyte	32.2 ± 5.9 (n = 19, 2689 points)
Alcian blue	P388D1	39.2 ± 5.0 (n = 17, 2571 points)

Erythrocytes or P388D1 cells were stained with ruthenium red or Alcian blue and processed for electron microscopy. Micrographs were digitized for computer-assisted determination of the mean apparent thickness of the electron-dense cell boundaries. Each value is a mean (± standard error of the mean) determined on a number n of different contact regions. The total number of points defined in these contours is also shown.

adhesion. It is concluded that the cell coat can in principle generate enough repulsive interactions to prevent repulsion. The key parameter is the relative length of adhesion molecules and repellers. The former is often well known due to reported structural studies made on individual receptor molecules. More quantitative information is needed on the thickness of the cell coats. The last point of concern is that estimates of repulsion forces or energies were obtained with equilibrium models. As emphasized by Israelachvili [30], hours may be required to achieve equilibrium configurations when polymer-coated surfaces are brought into close contact. Kinetic effects are thus to be expected, although our theoretical knowledge of cell surface structure and polymer dynamics may be insufficient to obtain safe theoretical estimates for these effects.

The second purpose of this work was to present some electron microscopical data concerning the thickness of the cell coat. Results suggested that macrophages and erythrocytes are coated with a glycocalyx with an apparent thickness on the order of 20–30 nm. These coats were found to be altered by adhesion. The closeness of apposition between membrane bilayers could be decreased either by increasing the adhesive stimulus or by decreasing surface charges. However, the significance of our results, and particularly the absolute value of the glycocalyx thickness, are hampered by at least five technical difficulties.

First, we do not know whether sample preparation for electron microscopy will preserve the glycocalyx thickness. Indeed, although the overall change of sample volumes is usually moderate [41], surface polysaccharides might display a peculiar behaviour in this respect. However, a recent comparison between the numerical values of cell substrate thicknesses as determined by interference-reflection microscopy and electron microscopy [42] suggested that the trend of intermembrane thickness variations might be preserved in electron microscopic studies. A clever way of circumventing this difficulty was found by Rutishauser who made cell aggregates in ferritin-containing medium and used the number of ferritin molecules trapped between apposed membranes as a marker of cell distance. However, the underlying assumption was

TABLE III Total membrane thickness in macrophages and erythrocytes after carbohydrate staining

	Free membrane thickness Erythrocyte	P388D1	Total membrane thickness Bound area Erythrocyte + P388D1
Glutaraldehyde-treated erythrocytes	22.1 ± 1.8 $n = 10$ 1525 points	31.5 ± 2.25 $n = 7$ 1011 points	19.0 ± 2.75 $n = 7$ 2501 points
Immunoglobulin-coated erythrocytes	18.5 ± 3 $n = 9$ 1223 points	28.3 ± 4 $n = 8$ 1285 points	22.5 ± 1.75 $n = 8$ 1039 points

Glutaraldehyde-treated or immunoglobulin-coated erythrocytes were bound by P388D1 cells. Samples were processed for electron microscopy, using ruthenium red to stain carbohydrates. The apparent thickness of cell boundaries was determined in free and contact areas. Mean values are shown together with standard error of the mean and number n of contact areas scanned in each case. The total number of points defined on boundaries is also indicated.

TABLE IV Effect of enzyme treatment on the uptake of opsonized erythrocytes by macrophages (static conditions)

Erythrocyte treatment	Adhesion efficiency (%)
Control	0
Antibodies	46
Neuraminidase (30 U)	1.8
Neuraminidase (3 U)	5.2
N-glycosidase	1.8
O-glycosidase	2.6
Neuraminidase (30 U) + antibodies	50
Neuraminidase (3 U) + antibodies	58
N-glycosidase + antibodies	28
O-glycosidase + antibodies	43

Suspensions of control and treated erythrocytes were deposited on monolayers of P388D1 cells. After incubation and washing, cells were examined microscopically for determination of the percentage of erythrocytes falling on a macrophage that were subsequentially bound.

TABLE V Effect of neuraminidase treatment on the uptake of opsonized erythrocytes by macrophages (dynamic conditions)

Erythrocyte treatment	Bound erythrocytes (%) (82 μm path, $G = 7\ s^{-1}$)	
Control	0	(0/154)
Antibodies	0	(0/113)
Neuraminidase (300 U)	0	(0/108)
Neuraminidase (30 U)	8	(11/133)
Neuraminidase (300 U + antibodies)	39	(21/54)
Neuraminidase (30 U + antibodies)	32	(13/41)

Control or treated erythrocytes were driven along monolayers of P388D1 cells in a parallel-plate flow chamber under microscopic control and videotape recording. Individual erythrocytes flowing on the bottom of the chamber were monitored for determination of the percentage of cells that were bound to the monolayer during their passage across the microscope field. Results are shown together with the number of binding and counted erythrocytes (in brackets).

that ferritin concentration should not be different near cell surfaces and in bulk medium.

Second, it is clear on electron micrographs that only a fraction of cell contours are actually involved in adhesion [35]. The simplest criterion used to define adhesive areas is to choose a threshold value for the interbilayer distance. This clearly sets a bias on the determination of mean cell–cell distances.

Third, the objective determination of the boundaries of electron-light or electron-dark areas around cell surfaces is not a trivial problem and sets a resolution limit to thickness determinations. According to our experience, the best way of defining cell contours was to draw them manually on enlarged digitized images.

Fourth, the actual thickness d of a three-dimensional sheet such as the cell membrane is usually different from the apparent thickness x measured on a micrograph. Indeed:

$$x = d/\cos\theta$$

where θ is the angle between the cell surface and the section plane. Both the mean value and standard deviation of x are dependent on the distribution of θ:

$$\langle x \rangle = d \int_0^{\pi} P(\theta)\, d\theta \qquad (3)$$

if the orientation of the plane is random, it is readily shown that:

$$P(\theta) = \sin\theta\, d\theta/2 \qquad (4)$$

which makes the right-hand side of Eqn. 3 a divergent integral. However, Eqn. 3 is wrong in view of the following argument: the probability that a random plane will cut a given contact area is proportional to the absolute value of $\cos\theta$ (where θ is the angle between the plane and the contact area); therefore, the probability that the angle between a random plane that cuts a contact area and this contact area be θ is:

$$P(\theta) = \sin\theta\, |\cos\theta| \qquad (5)$$

which yields, after straightforward integration:

$$\langle x \rangle = 2d \qquad (6)$$

There is still a bias in Eqn. 6, since areas of apposition between membranes may not be considered as contact areas when θ is markedly different from zero (since the apparent distance is high). Therefore, the average apparent thickness of a contact area probably lies between d and $2d$.

Fifth, although ruthenium red and Alcian blue are small molecules, the glycocalyx might act as a nucleation site for the binding of numerous electron-dense molecules, leading to an overestimate of the calculated

cell coat thickness. Conversely, it is not proven that all regions of the glycocalyx are properly stained. In particular, it is not proven that the glycocalyx is everywhere accessible to the dye. Thus, it is not too surprising that ruthenium red and Alcian blue yielded different images, and a proper calibration of the staining procedure is needed.

The third goal of this paper was to provide some experimental data concerning the effect of glycocalyx manipulation on adhesion. Our data strongly suggest the following points: cell coat repulsion effectively inhibited the interaction between macrophages and glutaraldehyde-treated erythrocytes under static conditions, suggesting that the equilibrium interbilayer distance was lower than the glycocalyx thickness. Repulsive forces were effective in preventing the interaction between phagocytes and immunoglobulin-coated red cells under dynamic, not static, conditions. This would be consistent with the view that (a) equilibrium interbilayer distance is higher with the latter erythrocyte type, and (b) repulsion is more important under dynamic than static conditions.

In conclusion, the above set of preliminary data strongly support the view that steric stabilization plays an effective role in modulating adhesion, and this is amenable to both structural and functional studies. More data are required to assess the generality of this concept.

References

1. A. CURTIS, "The cell surface: its molecular role in morphogenesis" (Logo Press, Academic Press, New York, 1967).
2. B. A. PETHICA, *Exp. Cell Res.* **Suppl. 8** (1961) 123.
3. H. JEHLE, *Ann. N.Y. Acad. Sci.* **158** (1969) 240.
4. T. A. SPRINGER, *Nature* **346** (1990) 425.
5. M. TAKEICHI, *Science* **251** (1991) 1451.
6. A. M. NORMENT, R. D. SALTER, P. PARHAM, V. H. ENGELHARD and D. R. LITTMAN, *Nature* **336** (1988) 79.
7. P.-Y. CHAN and T. A. SPRINGER, *Mol. Biol. Cell* **3** (1992) 157.
8. H. R. BAUMGARTNER, *Microvascular Res.* **5** (1973) 167.
9. M. B. LAWRENCE and T. A. SPRINGER, *Cell* **65** (1991) 859.
10. D. H. NAPPER, *J. Colloid & Interface Sci.* **58** (1977) 390.
11. *Idem.*, "Polymeric stabilization of colloid dispersions" (Academic Press, London, 1983).
12. P. G. DE GENNES, "Scaling concepts in polymer physics" (Cornell University Press, Ithaca, 1979).
13. *Idem.*, in "Physical basis of cell cell adhesion", edited by P. Bongrand (CRC Press, Boca Raton, 1988) p. 39.
14. A. MARTINEZ-PALOMO, *Int. Rev. Cytol.* **29** (1970) 29.
15. H. S. BENNETT, *J. Histochem. Cytochem.* **11** (1963) 14.
16. G. I. BELL, *Science* **200** (1978) 618.
17. P. BONGRAND, C. CAPO and R. DEPIEDS, *Prog. Surface Sci.* **12** (1982) 217.
18. P. BONGRAND and G. I. BELL, in "Cell surface dynamics: concepts and models", edited by A. S. Perelson, C. DeLisi and F. W. Wiegel (Marcel Dekker, New York, 1984) p. 459.
19. G. I. BELL, M. DEMBO and P. BONGRAND, *Biophys. J.* **45** (1984) 1051.
20. S. USAMI, S.-L. WUNG, B. A. SKIERCYINSKI, R. SKALAK and S. CHIEN, *ibid.* **63** (1992) 1663.
21. R. C. VALENTINE and N. M. GREEN, *J. Mol. Biol.* **27** (1967) 615.
22. M. V. NERMUT, N. M. GREEN, P. EASON, S. S. YAMADA and K. M. YAMADA, *EMBO J.* **7** (1988) 4093.
23. D. E. STAUNTON, M. L. DUSTIN, H. P. ERICKSON and T. A. SPRINGER, *Cell* **61** (1990) 243.
24. J. G. CYSTER, D. M. SHOTTON and A. F. WILLIAMS, *EMBO J.* **10** (1991) 893.
25. S. TIISALA, M. L. MAJURI, O. CARPEN and R. RENKONEN, *Scand. J. Immunol.* **39** (1994) 249.
26. U. RUTISHAUSER, A. ACHESON, A. K. HALL, D. M. MANN and J. SUNSHINE, *Science* **240** (1988) 53.
27. P. J. FLORY, "Principles of polymer chemistry", 11th Edn (Cornell University Press, Ithaca).
28. P. BONGRAND, in "Handbook of biophysics, vol. 1: Membranes I: structure and conformation", edited by R. Lipowsky and E. Sackmann (Elsevier, Amsterdam, 1994) in press.
29. A. K. DOLAN and S. F. EDWARDS, *Proc. Roy. Soc. A* **337** (1974) 509.
30. J. ISRAELACHVILI, "Intermolecular and surface forces" (Academic Press, New York, 1992).
31. L. A. SPIELMAN, *J. Colloid Interface Sci.* **33** (1970) 562.
32. P. BONGRAND (ed.) "Physical basis of cell–cell adhesion" (CRC Press, Boca Raton, 1988).
33. J. SCHLESSINGER, L. S. BARAK, G. G. HAMMER, K. M. YAMADA, I. PASTAN, W. W. WEBB and E. L. ELSON, *Proc. Natl. Acad. Sci. (USA)* **74** (1977) 2709.
34. G. BOUVIER, A. M. BENOLIEL, C. FOA and P. BONGRAND, *J. Leukocyte Biol.* **55** (1994) 729.
35. C. FOA, M. SOLER, M. FRATERNO, M. PASSEREL, J. L. LAVERGNE, J. M. MARTIN and P. BONGRAND, in "Studying cell adhesion", edited by P. Bongrand, P. Claesson and A. Curtis (Springer Verlag, Heidelberg, 1994) in press.
36. J. H. LUFT, *Anat. Record.* **171** (1971) 347.
37. J. L. MEGE, C. CAPO, A. M. BENOLIEL and P. BONGRAND, *Biophys. J.* **52** (1987) 177.
38. O. TISSOT, A. PIERRES, C. FOA, M. DELAAGE and P. BONGRAND, *ibid.* **61** (1992) 204.
39. A. PIERRES, O. TISSOT, B. MALISSEN and P. BONGRAND, *J. Cell Biol.* **125** (1994) 945.
40. C. CAPO, F. GARROUSTE, A. M. BENOLIEL, P. BONGRAND and R. DEPIEDS, *Immunol. Commun.* **10** (1981) 35.
41. M. V. KING, *Cell Biophys.* **18** (1991) 31.
42. J. P. HEATH, in "Cell behaviour", edited by R. Bellairs, A. Curtis and G. Dunn (Cambridge University Press, Cambridge, 1982) p. 77.

Received 4 May
and accepted 5 May 1995